Received: 27 October 2022 | Accepted: 2 June 2023

DOI: 10.1002/jpln.202200391

RESEARCH ARTICLE

Complementary effects of sorption and biochemical processing of dissolved organic matter for emerging structure formation controlled by soil texture

Franziska B. Bucka[1] | **Vincent J. M. N. L. Felde**[2] | **Stephan Peth**[2] | **Ingrid Kögel-Knabner**[1,3]

[1]Soil Science, Technical University of Munich, Freising, Germany

[2]Institute of Soil Science, University of Hanover, Hanover, Germany

[3]Institute for Advanced Study, Technical University of Munich, Garching, Germany

Correspondence
Franziska B. Bucka, Soil Science, Technical University of Munich, Emil-Ramann-Straße 2, 85354 Freising, Germany.
Email: franziska.bucka@tum.de

This article has been edited by Nadja Ray.

Funding information
Deutsche Forschungsgemeinschaft (DFG); MAD Soil—Microaggregates: Formation and Turnover of the Structural Building Blocks of Soils, Grant/Award Number: FOR2179

Abstract

Background: Percolating dissolved organic matter (DOM) from the topsoil is considered the main source of subsoil organic carbon (OC) in temperate soils, but knowledge about its influence on OC storage and structure-forming processes is limited.

Aims: We conducted a 30-day incubation experiment with artificial soils to study the effects of percolating DOM and soil texture on OC turnover and initial structure formation.

Methods: Artificial soils with contrasting texture, but identical mineral composition, were used to mimic subsoil conditions, where mineral surfaces free of OM come into contact with percolating DOM. After the incubation, we assessed the solution exchange, OM covers on minerals, microbial community and OC turnover, and aggregate formation and stability.

Results: A higher sand content caused a lower porosity, accompanied by a lower moisture content. In contrast, the OC retention (21% of the OC input), microbial activity, and community size were unaffected by soil texture. The OM covered 10% of the mineral surfaces within an otherwise OC-free mineral matrix. The formation of large, water-stable aggregates occurred in all soils, but was pronounced in the clay-rich soils (58% mass contribution), which also supported a higher mechanical stability of the aggregates.

Conclusions: The initial retention and microbial mineralization of DOM are decoupled from pore sizes and soil solution exchange but are driven by the mineral composition and OC input. The biochemical processing of the percolating DOM can induce large aggregates. Here, the presence of fine mineral particles enhances the formation and mechanical stability of the aggregates, irrespective of their surface charge or sorptive properties.

KEYWORDS
aggregate formation, deep soil, dry-crushing, microcosm experiment, PLFA analysis, specific surface area

1 | INTRODUCTION

Soils harbor the majority of the terrestrial organic carbon (OC) (Jobbágy & Jackson, 2000) and serve humanity in many different ways since thousands of years, for example, by providing the basis for agricultural food production. The physical structure of a soil is considered a key factor defining its functionality and agricultural usability (Dexter, 1988). The spatial arrangement and stability of the organic and mineral soil components have significant effects on plant development, water balance, and soil workability (Dexter, 1988). Furthermore, soil erodibility is closely related to its structural stability (Barthès & Roose, 2002).

Besides the abiotic aspects, the formation and stabilization of soil structure is often investigated with respect to the role of organic matter (OM) (Bucka, Pihlap, et al., 2021; Christensen, 2000; Franzluebbers, 2002; Lehmann et al., 2008; Tisdall & Oades, 1982). Soil organic matter (SOM) can stabilize soil structure in many ways, for example, by organic debris serving as nuclei for subsequent attachment of minerals or extracellular polymeric substances (EPS) gluing mineral particles together (Totsche et al., 2018). Because agricultural practices and plant growth are mostly limited to the upper soil horizons, most of the research has focused on processes within topsoils (Amézketa, 1999; Dexter, 1977; Tisdall, 2020). As a consequence, the effect of particulate OM on soil structure formation and OM storage has been studied extensively, as this is considered to be the main source of OM in topsoils (Kögel-Knabner, 2002; Mikutta et al., 2019; Sokol et al., 2019; Witzgall et al., 2021). In contrast, the deeper parts of the soils have only fairly recently gained interest with respect to OM storage and turnover (Chabbi et al., 2009; McCarthy, 2005; Rumpel et al., 2012). Although subsoils have usually a low OM content, they may still store the majority of total soil organic carbon (SOC) because of their large depth (Batjes, 1996; Jobbágy & Jackson, 2000; Lorenz & Lal, 2005). Jobbágy and Jackson (2000) estimated that 60% of the global SOC stocks of 2344 Pg are stored below 40 cm soil depth.

The OM input to subsoils is mainly delivered by plant roots and percolating dissolved organic matter (DOM) (Angst et al., 2016; Angst et al., 2018; Rumpel et al., 2012; Rumpel & Kögel-Knabner, 2011), with the latter being considered to be the main source of subsoil OM in temperate soils (Ahrens et al., 2015; Kaiser & Kalbitz, 2012; Kalbitz et al., 2000).

DOM is an operationally defined collective term describing OM <0.45 μm, which can originate from plant litter, microbial biomass, or root exudates (Kalbitz et al., 2000). Depending on its origin, it contains a varying amount of nutrients (Meyer et al., 2018) and OC bound within complex molecules like organic acids, sugars, and amino acids, all of which can be used as substrate by microorganisms (Kaiser et al., 2004; Kaiser & Kalbitz, 2012; Liu et al., 2019; Qualls & Haines, 1992).

Although the depth of the direct influence by roots is limited to the extension of the root system, percolating DOM from upper soil horizons can transfer OC into much deeper soil regions. This depth migration is dependent of the water flow in the vadose zone and OC retention at mineral surfaces (Krettek & Rennert, 2021; McCarthy, 2005; Merdy et al., 2021), implying that soil texture can have a major influence on OC mobility.

Because of the overall low OC concentration and pedogenic mineral formation at the weathering front, the subsoil mineral surfaces are mostly free of OM and prone to adsorb OC (Kaiser & Guggenberger, 2003; Kaiser & Kalbitz, 2012). Percolating DOM through soil pores can come into contact with the mineral surface and therefore a large proportion of the SOM in deep subsoils is stored in organo-mineral associations (Angst et al., 2018; Kögel-Knabner & Amelung, 2021). Although DOM adsorption to mineral surfaces has been extensively studied, it is necessary to think beyond those processes by including the aspects of OM storage and turnover under flow conditions taking into account the processes of soil structure formation. In soils, DOM does not only undergo processes of adsorption and desorption, but the formed organo-mineral associations can lead to soil aggregation and structural development. Understanding these processes can lead to a more holistic and process-related understanding of OC storage and structure formation in subsoil systems.

A previous incubation experiment with artificial soils (composed of a mineral mixture mimicking a temperate Cambisol without preexisting soil structure) could show that initial structure formation via the interaction between OM and minerals is possible by microbial processing of an OC-rich solution without requiring the presence of particulate OM nuclei (Bucka et al., 2019). However, understanding the processes of the DOM-induced structure formation requires a systematic investigation of the soil texture effect on OC mobility and storage, microbial life, and aggregate formation. It is especially necessary to differentiate between the effect of the grain size and the sorptive properties of minerals.

In this study, we conducted a short-term laboratory incubation experiment to investigate the initial processes of DOM-induced soil structure formation. We used artificial model soils, designed with contrasting textures, but identical mineral composition to disentangle the effect of texture (i.e., grain size) from that of the mineral composition (i.e., clay mineral surface) of a soil. The mineral mixtures mimicked the characteristics of subsoils had no preexisting soil structure and initially OC-free mineral surfaces. The application of a constant suction head throughout the experiment enabled the DOM to percolate freely through the soil matrix. After the incubation, we analyzed the water balance, OC turnover, microbial activity, and community composition, and assessed the effect of DOM on soil structure formation and stability.

2 | MATERIAL AND METHODS

2.1 | Artificial model soils and dissolved organic matter

The artificial model soils were based on a mineral mixture with three contrasting textures: (1) clay loam (31% clay, 48% silt, and 21% sand), (2) loam (16% clay, 39% silt, and 45% sand), and (3) sandy loam (12% clay, 15% silt, and 73% sand). The soils were mixed in a dry state by adding the components step by step from coarser to finer particle size followed by 2 h shaking in an overhead shaker. The mineral

mixtures consisted of 89 wt% quartz in clay, silt, and sand size (Euroquarz, Laußnitz, Germany), 7 wt% illite (Aspanger, Aspang, Austria), 3 wt% montmorillonite (Franz Mandt, Wunsiedel, Germany), and 1 wt% goethite (Sigma-Aldrich, Steinheim, Germany). The cation exchange capacity of the clay fraction was 37 ± 1 $cmol_c\ kg^{-1}$, with the main exchangeable cations being Ca^{2+} (62%), K^+ (22%), and Mg^{2+} (14%). The percentage of montmorillonite, illite, and goethite was kept constant, whereas the percentage of clay-, silt-, and sand-sized quartz was varied to produce the different soil textures in order to disentangle the effect of the grain size from that of the clay minerals.

The soils were inoculated with a microbial inoculum isolated from an arable Cambisol by water-extraction according to Lehmann et al. (2018), and Pronk et al. (2012), using the extract of 1.2 g soil per microcosm as described in Bucka et al. (2019). The DOM solution was prepared by water-extraction of milled hay litter (hay:water, 1:20, w:w) produced from grass-clover hay (*Trifolium* spec., *Lolium perenne* L., *Lolium multiflorum* L., organic farming, 41% OC, C:N ratio 29). The hay-water suspension was shaken, incubated at 35°C for 48 h (Phoenix Instrument, Garbsen, Germany), and subsequently filtered to <0.45 µm by pressure filtration. The OC concentration was 4 mg OC mL^{-1} with a molecular characterization of 66% O/N-alkyl-C, 13% alkyl-C, 12% aryl-C, and 9% carboxyl-C (Supporting Information 1), and the macromolecular composition consisted of carbohydrates (50%), lignin (24%), carbonyl (10%), proteins (8%), and lipids (8%) (molecular mixing model; Supporting Information 1). The elements in the DOM solution were mostly K, Ca, P, Mg, and S, indicating a high nutritive quality (Supporting Information 2).

2.2 | Microcosm incubation

The incubation was done in individual microcosms (unplasticized PVC, diameter 8.1 cm, height 9.1 cm; fill level depending on bulk density, 4.2 cm for the sandy loam, 4.4 cm for the loam, 5.5 for clay loam), filled with 300 g of dry artificial soil mixture (3 replicates of each texture), according to the setup described in Bucka et al. (2019). For the incubation, the microcosms were placed onto a suction plate (plastic suction plate with polyamide membrane, pore size 0.45 µm, ecoTech Umwelt-Messsysteme, Bonn, Germany), which ensured a constant suction pressure of −15 kPa (corresponding to pF 2.2) throughout the 30-day incubation period. The microcosms either received DOM solution in regular additions (treatment) or the same amount of solution without OM (control) with three replicates each. The solutions were added in portions of 10 mL every second day (15 mL during the first 4 days for initial wetting), leading to 195 mL of solution in total. The solutions where either a Hoagland's solution (1:10 diluted, pH 5.5, Hoagland's No. 2 basal salt mixture, Sigma-Aldrich, Steinheim, Germany) for the control group, or the DOM solution—including the equivalent amount of Hoagland's solution—for the treatment group. The solution was added drop by drop onto the microcosm's surface using a syringe (volume 5 mL, input precision 10 ± 0.03 mL) with cannula (20 gauge) to avoid impact or sealing of the surface as much as possible. The moisture content of the soils was determined by weighting the microcosms 24 h after each irrigation.

The initial OC content of the mineral mixtures including the microbial inoculum was <0.35 mg OC g^{-1} soil and the DOM input accounted for 2.6 mg OC g^{-1} soil. The OC input simulated the amount of DOM that can be leached from fresh POM litter in natural soils (Hagedorn & Machwitz, 2007). The overall OC input was determined by the total amount of solution and the maximum OC concentration therein, which we assumed to reflect the input of natural soils.

The released CO_2 during the incubation was monitored twice a week according to the method by Isermeyer (1952) adapted by Bimüller et al. (2014) and Bucka et al. (2019). For this purpose, the microcosms were placed for 5 h into an airtight container, in which the released CO_2 was trapped with sodium hydroxide solution and afterward determined by titration with hydrochloric acid.

After the incubation, the soils were harvested and divided into three different aliquots (approx. 80 g for each fraction): (1) fresh material, short-term stored at 4°C for aggregate fractionation; (2) air-dried material for OC and N analysis, OC coverage, and mechanical stability tests of the aggregates; (3) freeze-dried material for phospholipid fatty acids (PLFA) extraction.

2.3 | Porosity

The total porosity (n) was calculated using the data of the bulk density (d_B) and literature values for particle density (d_P, 2.65 g cm^{-3} for the quartz, 2.7 g cm^{-3} for the illite, 2.35 g cm^{-3} for the montmorillonite, and 4.3 g cm^{-3} for the goethite) according to the following equation (1):

$$n = 1 - \frac{d_B}{d_P}. \quad (1)$$

The proportion of the water-filled pore space (WFPS, %) was calculated using the moisture content (V_w; cm^3) and the total porosity (V_V; cm^3) according to the following equation (2):

$$WFPS = \frac{100}{V_V} \times V_W. \quad (2)$$

The water-filled pores had an equivalent diameter of <20 µm at the adjusted matric potential of −15 kPa. The pore diameter has been calculated according to the Young–Laplace-equation for capillary rise under the assumption that the pores function as a bundle of cylindrical capillaries with distinct radii and circular water menisci (described in Tuller et al., 2004) according to Equation (3), where r is the capillary radius (m), γ is the surface tension (N m^{-1} at 20°C), α is the contact angle, h is the capillary rise (m), p is the water density (kg m^{-3}), and g is the gravitational acceleration (N kg^{-1}).

$$r = \frac{2 \times \gamma \times \cos\alpha}{h \times p \times g}. \quad (3)$$

A higher proportion of WFPS implies a pore system dominated by smaller pores, as there are more water-filled pores present at the same matric potential.

2.4 | OC coverage

The specific surface area (SSA) was determined by multipoint N_2-Brunauer–Emmett–Teller (BET) according to the BET method (Brunauer et al., 1938). The SSA of the air-dry soil was measured by N_2 adsorption at 77 K according to the description in Heister (2016). Assuming that the mineral surfaces covered with OM are negligible in the N_2-BET measurement (Heister, 2014), the OC covered surface area was calculated by subtracting the SSA of the soils with DOM from the SSA of the respective control mixtures without DOM.

The established mineral–mineral surface interactions through dry-mixing and incubation of the pure mineral mixtures were assessed by subtracting the SSA of the control soils (before and after incubation) from the summed up SSA of the soil components.

2.5 | OC content, allocation, and characterization

The OC and N content of the bulk soil and aggregate fractions were determined by dry combustion with a CN analyzer (HEKAtech, Wegberg, Germany) using approximately 20 mg of air-dry sample material (ground to a fine powder).

The amount of OC leached during the incubation was calculated by subtracting the bulk soil OC content after the incubation and the released CO_2–C from the total OC input.

The molecular characterization of a freeze-dried aliquot of the DOM solution was measured by solid-state ^{13}C-NMR spectroscopy (Bruker, Rheinstetten, Germany) using cross-polarization magic angle spinning at 6.8 kHz with 1 ms contact time and 1 s pulse delay (Schaefer & Stejskal, 1976). Four chemical shift regions were integrated within the spectrum to calculate the relative abundance of alkyl C (0–45 ppm), O/N-alkyl C (45–110 ppm), aryl C (110–160 ppm), and carboxyl C (160–220 ppm) (Knicker et al., 2005; Wilson, 1987). The molecular mixing model by Nelson and Baldock (2005) was applied to determine the proportions of the abundant biomolecules (carbohydrate, protein, lignin, lipid, carbonyl, and char).

2.6 | Microbial community composition

The microbial community composition was analyzed by using PLFA as described in Frostegård et al. (1991). The extracted lipids were determined as fatty acid methyl esters by gas chromatography with flame ionization detection (Thermo Fisher Scientific, Waltham, USA) with a silica capillary column (Phenomenex Ltd., Aschaffenburg, Germany) according to Baumert et al. (2018) and Bucka, Felde et al. (2021). The PLFAs were assigned to microbial groups according to Frostegård et al. (1991, 1993): 15:0, 17:0, a15:0, i15:0, i16:0, i17:0, 16:1ω7, cy17:0, and cy19:0 are of bacterial origin, including gram-positive bacteria (a15:0, i15:0, i16:0, i17:0) and gram-negative bacteria (16:1ω7, cy17:0), and 18:2ω6 is of fungal origin. Some PLFAs (14:0, 16:0, 18:0, 20:0, and 18:1ω9t) were not assigned to one microbial group but were still considered to be of microbial origin, leading to a total of 15 PLFAs used for the calculation of the total PLFAs. The ratios of fungal to bacterial PLFAs and gram-positive to gram-negative PLFAs were used as an indicator for differences in the composition of the developed microbial community.

2.7 | Aggregate fractionation

The aggregate size distribution was determined by submerged sieving of the soils before and after the incubation. Approximately 15 g of moist soil was placed on a sieve stack (630, 200, and 63 µm sieve), submerged in deionized water and sieved for 2 min at 0.5 Hz (1 cm upstroke). The sieve fractions were oven-dried at 60°C for approx. 24 h and weighed to calculate the mass contribution of the four size fractions (large macroaggregates [>630 µm], small macroaggregates [630–200 µm], large microaggregates [200–63 µm], and small microaggregates [<63 µm]). There was no correction for the sand content in the macroaggregate fraction, as the known texture of the mineral mixtures allowed to calculate the overall mass increase due to the storage of finer particles in this fraction after the incubation.

2.8 | Aggregate dry-crushing

The mechanical stability of the aggregates was tested by dry-crushing with a mechanical loading frame (ZwickRoell, Ulm, Germany). Air-dry aggregates (4–2 mm) were crushed by a piston moving continuously (500 µm min^{-1}) from 4.1 mm toward 1.5 mm distance to the compression table as described in Bucka, Felde et al. (2021). The force applied during crushing was recorded with a high-resolution load cell ("Xforce HP" 100 N load cell, ZwickRoell, Ulm, Germany) as described in Felde et al. (2021).

The applied work for a size deformation to 80% of the aggregates original size was calculated (area of the force–displacement curves) and normalized to the aggregate diameter (mJ m^{-1}) as described in Bucka, Felde et al. (2021). The number of force drops (local maxima of the force–displacement curves) of various magnitudes (>5%, >10%, >25%, >40%, >50%, >75%) was counted to record aggregate failures of different magnitudes during the crushing process.

2.9 | Statistical analyses

The effect of the soil texture and DOM input was tested for statistical significance for the data of soil moisture content, pore space characteristics (total porosity and WFPS), OM coverage of the mineral surfaces, OC concentration of the bulk soils and aggregates, OC respiration (CO_2–C), the aggregates' mean weight diameter and mechanical stability (applied work and force drop counts), and the microbial community structure (PLFA, fungal:bacteria ratio, gram positive:gram negative bacteria ratio). For testing the statistical significance, a one-way ANOVA was applied in combination with a post hoc Tukey HSD test in R (R Core Team, 2017). Prior to testing, the datasets were tested

TABLE 1 Soil moisture content, porosity, and water-filled pore space of the soils, OM coverage on mineral surface (percent values give coverage as proportion of total mineral surface).

	Soil moisture (vol%)		Porosity (vol%)		Water-filled pores (% pore volume)		OM coverage ($m^2\ g^{-1}$)
	Control	DOM	Control	DOM	Control	DOM	
Clay loam	36 ± 1*a*	35 ± 2*a*	60 ± 0*a*	62 ± 2*a*	60 ± 1*a*	56 ± 4*a*	1.0 ± 0.1*a* (11%)
Loam	28 ± 1*b*	27 ± 1*b*	52 ± 0*a*	55 ± 0*b*	54 ± 1*a*	49 ± 1*a*	0.50 ± 0.2*b* (9%)
Sandy loam	17 ± 1*c*	18 ± 1*c*	49 ± 1*c*	49 ± 1*c*	34 ± 2*b*	37 ± 1*b*	0.53 ± 0.2*b* (11%)

Note: Data are given as mean values ± standard deviation, lowercase italic letters indicate significant effects of the soil texture ($p < 0.05$).
Abbreviation: DOM, dissolved organic matter.
Source: *Data from Bucka et al. 2021.

TABLE 2 Organic carbon (OC) allocation between the bulk soil OC, respired OC, and leached OC before and after the incubation.

	OC initial	OC input	OC end		CO2–C respired		OC leached	
		DOM	Control	DOM	Control	DOM	Control	DOM
Clay loam	0.33 ± 0.01	2.6	0.15 ± 0.02	0.72 ± 0.10*a*	0.03 ± 0.02	0.42 ± 0.07*a*	0.15 ± 0.05	1.79 ± 0.18*a*
Loam	0.32 ± 0.11	2.6	0.19 ± 0.02	0.68 ± 0.13*a*	0.09 ± 0.05	0.44 ± 0.05*a*	0.03 ± 0.17	1.79 ± 0.29*a*
Sandy loam	0.22 ± 0.00	2.6	0.21 ± 0.00	0.71 ± 0.02*a*	0.09 ± 0.02	0.44 ± 0.04*a*	-0.09 ± 0.03	1.67 ± 0.07*a*

Note: Data are given as mean values in the unit mg g^{-1} soil ± standard deviation, lowercase italic letters indicate significant effects of the soil texture ($p < 0.05$).
Abbreviation: DOM, dissolved organic matter.

for normality and homoscedasticity by applying the Shapiro–Wilk test and a graphical inspection of the QQ-plots, and the Bartlett test or Levene's test for non-normal distributed data. If the requirements for parametrical testing were not met, a Kruskal–Wallis test was applied. A significance level of $\alpha = 0.05$ was defined for all tests. The data analysis was done with the statistical software R (R Core Team, 2017, version 4.2.1, with the packages *stats* and *agricolae*), within the RStudio environment.

3 | RESULTS

3.1 | Pore space and soil moisture content

The texture defined the bulk density and total pore space, causing the highest bulk density and lowest porosity in the sand-rich mixtures (Table 1). Accordingly, the moisture content in the microcosms was lowest in the sandy loam (17 vol%) and highest in the clay loam (36 vol%; $p < 0.001$). The WFPS accounted for 60% in the clay loam, whereas it accounted for 34% in the sandy loam, indicating a pore system with more coarse pores (>20 μm) in the sand-rich soils, as expected. The DOM input had no significant effect on those properties ($p = 0.3772$), but slightly increased the moisture content and WFPS in the sand-rich soil, especially at later stages of the incubation (Supporting Information 3).

3.2 | OC turnover and coverage of mineral surfaces

The bulk OC content after the incubation was similar for all textures (0.7 ± 0.02 mg C g^{-1} soil, Table 2). During the incubation, approximately 0.43 ± 0.01 mg CO_2–C g^{-1} soil was released from all microcosms, regardless of the texture (Table 2). According to the total OC input of 2.6 mg OC g^{-1} soil, 27% of the OC was retained in the microcosms, 15% was released as CO_2, and 58% was leached.

After the incubation, 0.5–1 m^2 surface area per g mineral mixture was covered by OM (Table 1). The clay-rich mixture had largest total OM covers (1.0 ± 0.1 $m^2\ g^{-1}$), but the proportion of the covered surface corresponded to approximately 10% of the available surface area in all textures.

The mineral–mineral interactions accounted for the majority of the mineral surface coverage. The dry-mixing and incubation of the control soils (without DOM) caused a mineral surface coverage of 3.4 $m^2\ g^{-1}$ in the clay loam, 4.0 $m^2\ g^{-1}$ in the loam, and 4.0 $m^2\ g^{-1}$ in the sandy loam by mineral–mineral interactions (accounting for approximately 30%, 49%, and 55% of the total mineral surface).

3.3 | Development of the microbial community

The total amount of extracted PLFA was unaffected by the texture and yielded in 97 ± 6 nmol g^{-1} soil (Table 3). The contrasting textures did not lead to significant differences in the microbial community composition (total PLFA: $p = 0.958$; fungal:bacterial PLFA: $p = 0.514$; gram positive:gram negative bacterial PLFA: $p = 0.811$). The microbial community composition was dominated by bacteria, with a fungi:bacteria PLFA ratio ≤0.05 in all microcosms (Table 3). A higher sand content induced a slightly higher fungi:bacteria PLFA ratio, indicating a higher relative proportion of fungi. A higher sand content led also to a slightly higher proportion of gram-positive bacteria, as the ratio of gram positive:gram negative PLFA increased with higher sand-content

TABLE 3 Phospholipid fatty acids (PLFA) pattern of the soils after incubation.

	Total extracted PLFA (nmol g^{-1})	fungal:bacterial PLFA ratio	gram positive:gram negative PLFA ratio
Clay loam	104.1 ± 8.2*a*	0.02 ± 0.01*a*	0.71 ± 0.09*a*
Loam	92.7 ± 15.7*a*	0.03 ± 0.02*a*	0.76 ± 0.17*a*
Sandy loam	93.4 ± 11.6*a*	0.05 ± 0.03*a*	1.14 ± 0.15*a*

Note: Data are given as mean values ± standard deviation, lowercase italic letters indicate significant effects of the soil texture ($p < 0.05$); there were no significant differences between the soil textures (total PLFA: $p = 0.958$; fungal:bacterial PLFA: $p = 0.514$; gram positive:gram negative bacterial PLFA: $p = 0.811$).

(0.71 ± 0.09 in the clay loam, 0.76 ± 0.17 in the loam, and 1.14 ± 0.15 in the sandy loam).

3.4 | Aggregate formation and OC allocation

The DOM input induced the formation of water-stable aggregates in all microcosms, with strongest effects in the clay-rich textures (Figure 1A). The overall aggregate formation could be shown by the increase in mean weight diameter of the aggregates (Figure 1B; $p < 0.001$).

There was the predominant formation of large macroaggregates, with a mass contribution increase of up to 0.5 g g^{-1} in the clay loam, leading to an increase in the mean weight diameter by almost 60% (Figure 1B). In the sandy loam, the increase was lower (23%) but still caused 49% of the particle mass to be found in the large macroaggregate fraction (compared to 25% in the preincubation state).

The mass of all other size fractions was reduced after the incubation, except for the large microaggregate size in the loam texture, in which the DOM input induced a particle transfer (mass increase of 0.05 g g^{-1}).

The macroaggregate fractions had overall the same OC concentration (mean value of all textures 0.7 ± 0.1 mg OC g^{-1} soil) as the bulk soil (Figure 2), with the small macroaggregate fractions being even slightly depleted in OC (mean value of all textures 0.4 ± 0.2 mg OC g^{-1} soil). In contrast, the microaggregate fractions were enriched in OC. There was a strong OC enrichment in the large microaggregate fraction in all textures (mean value of all textures 1.9 ± 0.3 mg OC g^{-1} soil). In the small microaggregate fractions, a higher sand content led to a stronger OC enrichment (0.6 ± 0.1 mg OC g^{-1} soil in the clay loam, 1.4 ± 0.2 mg OC g^{-1} in the loam, and 3.2 ± 0.3 mg OC g^{-1} soil in the sandy loam).

3.5 | Mechanical stability and crushing pattern of the aggregates

The physical work necessary to crush the clay loam aggregates down to 80% of their original size was 0.11 ± 0.01 mJ mm^{-1}, whereas 0.09 ± 0.01 mJ mm^{-1} was necessary for the loam aggregates, and 0.06 ± 0.03 mJ mm^{-1} was already enough to crush the sandy loam aggregates (Figure 3A). This suggests that higher clay content led to an increased mechanical stability of the aggregates, although the effect was not significant ($p > 0.05$). The breakdown patterns showed more small force drops (>5%) with higher clay content, but more large force drops (>40%) with higher sand content (Figure 3B), indicating a higher number of large cracks during the breakdown of the sand-rich aggregates.

4 | DISCUSSIONS

4.1 | The mineral matrix regulates interactions between sorbent and adsorbate

Our experimental setup aimed at mimicking the unsaturated flow conditions of natural subsoils, in which OC-free mineral surfaces come into contact with percolating dissolved OM. The soil texture defined the flow characteristics and water balance of the soils. A higher sand content was accompanied by an overall lower porosity, but larger size of the individual pores (Table 1), leading to lower moisture content at the applied suction head of −15 kPa throughout the experiment. Because all microcosms were irrigated with the same amount of solution, it implies a lower liquid retention and a faster exchange of the soil

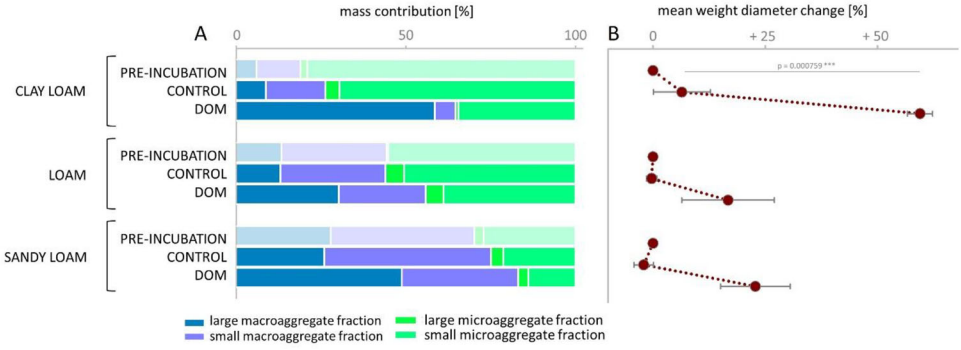

FIGURE 1 Aggregate formation as shown by the mass contribution of the size fractions (A) in comparison to the control soils and the preincubation state of the mineral mixtures. Changes in the mean weight diameter due to the maturation (related to the preincubation state) (B).

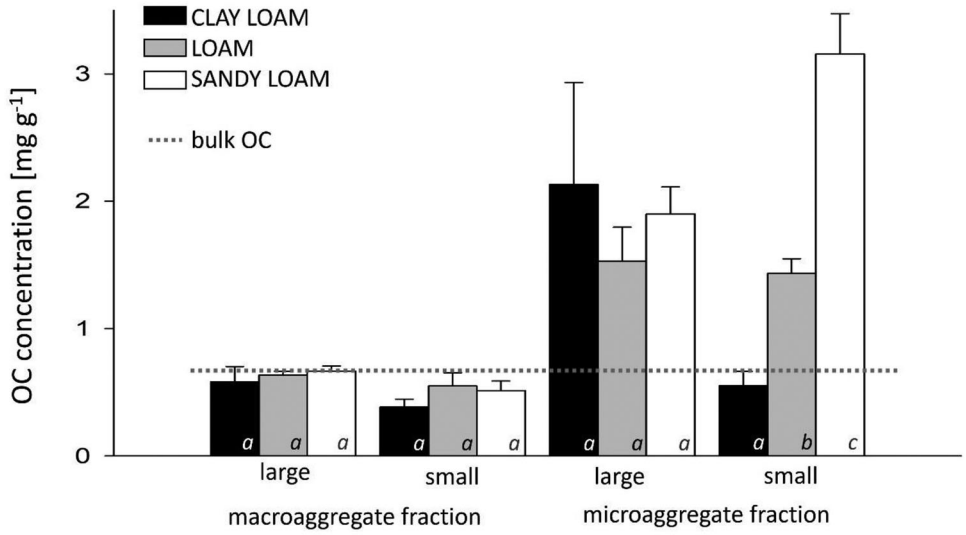

FIGURE 2 Organic carbon (OC) concentration in the aggregate fractions. The dotted line indicates the OC concentration in the bulk soil; OC concentration in the aggregates above that line indicate a relative OC enrichment of the aggregate fraction compared to the bulk soil. Data are given as mean values, the error bars display the standard deviation, and lowercase italic letters indicate a significant effect of the soil texture ($p < 0.05$).

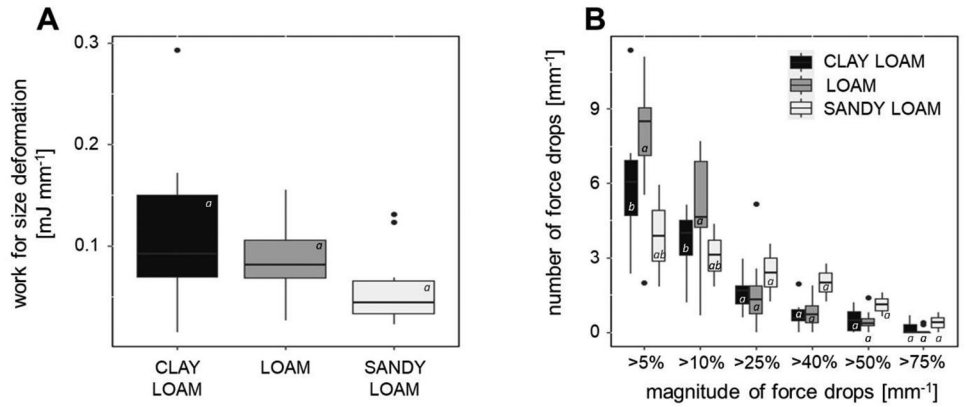

FIGURE 3 Mechanical stability parameters of the aggregates as obtained by dry crushing: (A) work for a deformation to 80% of the aggregates' original size and (B) force drops during the crushing process. Lowercase italic letters indicate a significant effect of the soil texture ($p < 0.05$).

solution in the sand-rich soils. As a result, five portions of DOM solution would theoretically have been sufficed to replace the whole soil solution in the sand-rich soil, whereas more than twice as many (11) portions would have been needed in the clay-rich soil.

Although the soil texture defined the pore space and the soil solution, the OC retention (analyzed after the incubation) was unaffected by the soil texture. Despite the differences in the solution exchange and clay-sized particle content, the OC content after the incubation was the same for all soils (0.7 ± 0.2 mg OC g^{-1}; corresponding to 21% of the OC input; Table 2). The similar OC retention in all soils at the end of the experiment was an unexpected result, because a finer soil texture used to be associated with more OC retention, which is attributed to the larger surface area available for sorption (Nelson et al., 1992; Shen, 1999).

This leads to the conclusion that the effective OC retention from dissolved OM is decoupled from the movement of the soil solution. A possible explanation lies in the strength of the interactions between the mineral surfaces and OM molecules. In soils, the mineral matrix, namely, the edges of layered silicates and quartz grains, as well as metal oxides and hydroxides, is considered to contribute to the DOM sorption (Inagaki et al., 2020; Kaiser et al., 1997; Kalbitz et al., 2000; Mikutta et al., 2007). Different soil minerals may sorb DOM to different degrees. A column experiment by Weigand and Totsche (1998) showed a weak and reversible DOM retention by quartz grains alone, whereas goethite coatings on quartz induced a stable OC retention. In addition, a batch experiment by Kahle et al. (2003) highlighted the importance of illite for DOC retention. In our experiment, the fraction of montmorillonite, illite, and goethite was kept constant, whereas

the amount of clay-sized quartz was varied to produce the different soil textures. The used mineral composition differed from that of natural soils but allowed us to distinguish between the effect of grain size and that of clay mineral surfaces. In our soils, there was an identical amount of potential absorbent for stable OC adsorption, which can explain the texture-independent OC content in the soils after incubation. In the finer soil texture, there was a higher amount of clay-sized quartz, which increased the total available surface area, but diluted the "reactive" mineral surface area that is responsible for stable OC adsorption.

Assuming that the effectively retained OC after the incubation was predominantly adsorbed to the clay minerals and goethite, the retained OC (0.7 mg C g^{-1} soil) corresponds to 0.16 mg C m^{-2}. This coverage is below any reported adsorption maxima, which are between 0.2 and 4 mg C m^{-2} for clay minerals and iron oxides (Kalbitz et al., 2000; Wagai et al., 2009). We measured a coverage of approximately 10% of the mineral surface by OM in our experiment (Table 1). This underlines the growing evidence that soil mineral surfaces are rarely fully occupied by OC, which has been both proven for batch experiments (Kahle et al., 2003), as well as for natural podzolic B-horizons (Wagai et al., 2009). With our simulated subsoil environment, we close the gap between batch experiments and natural soil samples. We show that under unsaturated flow conditions, the percolating DOM creates patches of adsorbed OM, providing OC, nutrients, and moisture, which predetermines the spaces for subsequent microbial colonization.

Those OC patches are possibly located in the preferential flow paths created by the initial wetting of the soil mixtures. When unstructured mineral soils are rapidly wetted, paths of preferential flow are created by the percolating wetting front (Dekker & Ritsema, 2000; Morales et al., 2010). Micro-CT scans of an artificial soil with loamy texture in a previous experiment revealed a significant formation of large macropores during maturation (Bucka et al., 2019). We assumed those macropores to reflect initially formed regions of preferential flow, which result in an inhomogeneous moisture and substrate distribution and subsequently define which particle surfaces come into contact with DOM. The particle surfaces facing the pore lumen are potential absorbents for the molecules of the DOM solution, whereas the vast mineral matrix might not get into contact with the OC initially introduced by the DOM.

Our experimental design allowed to disentangle the effects of particle-size from the sorptive properties of the minerals. Although the soil texture defined the size of the pore space and the amount of retained soil solution, it did not affect the effective OC retention, implying that the effective OC retention from dissolved OM is decoupled from the movement of the soil solution. A fine soil texture creates a finer pore system, which enables more soil solution storage, whereas a larger grain size allows a faster soil solution exchange. However, the OC storage relies on the mineral composition and is therefore decoupled from pore sizes and soil solution exchange. A higher amount of clay-sized quartz hereby "dilutes" the mineral surface area of clay minerals that is available for OM sorption.

4.2 | Microbial OM turnover is independent of the soil texture

Approximately 15% of the OC input was respired as CO_2 in all soils during the incubation (Table 2), suggesting that the microbial OC mineralization was independent of the soil texture. This means that the OC availability for the microorganisms was neither affected by the grain size of the mineral particles nor by the different pore sizes.

The texture-independent mineralization rates, as observed in our experiment, are in contrast to the reduced mineralization rates usually observed in soils with higher clay contents (Amato & Ladd, 1992; Hassink, 1997; Ladd et al., 1985; Sørensen, 1972; Thomsen et al., 1999). In those experiments, the limited accessibility of the OM due to the finer pore system, and entrapment of OC within the aggregates of clay-rich soils has been used as an explanation. However, all those experiments focused on the decomposition of particulate OM in agricultural topsoils. In our experimental set up though, subsoil conditions were mimicked with no preexisting aggregates, and microorganisms that have been introduced by a liquid inoculum. This means that the microorganisms probably come into contact with the percolating DOM delivering OC and nutrients to the pores established by the preferential flow. Therefore, the OC availability for the microorganisms may not be hampered by limited access through fine pores, as it may be the case for particulate OM within a clay-rich topsoil. Thus, it seems likely that the OM decomposition in subsoils is controlled by different factors than in topsoils. In topsoils, the decomposition is regulated by the physical substrate accessibility (Ladd et al., 1985), whereas for subsoils the limiting factor is not the accessibility, but the amount of OC and nutrients introduced by the percolating DOM. Consequently, the clay content and the available mineral surface area are not restricting microbial OC degradation in subsoils at early stages of the soil development.

Although there were no significant differences in the microbial community composition for the different mixtures, there was a trend toward a higher proportion of fungi and gram-positive bacteria in the sand-rich soils (Table 3). Gram-positive bacteria have a thick peptidoglycan cell wall layer, providing a higher drought-resistance (Schimel et al., 2007). This drought resistance might be a competitive advantage in sand-rich soils, in which the coarse pores and low moisture content probably reduced the overall water-availability for microorganisms. Fungi are also known to be able to explore larger air-filled pores (Otten et al., 1999; Soufan et al., 2018). Although the experiment was conducted under well-watered conditions, there was a faster soil solution exchange in the sand-rich soils. Hence, the microorganisms needed to invest into the release of EPS, to modulate their environment with respect to trap nutrients and OC of the percolating DOM (Costa et al., 2018; Flemming & Wingender, 2010). The higher content of WFPS in the sand-rich soils after DOM addition (Table 1) hints toward the presence of those EPS increasing water retention in the soil by reducing the connectivity of the pore space and thereby cause an increased water-holding capacity (Benard et al., 2019; Costa et al., 2018; Roberson & Firestone, 1992).

Our experiment showed that in subsoils, where the main OM input is in form of percolating DOM, soil texture and the corresponding pore system have no effect on the microbial OC turnover. On the contrary, the initial OC turnover seems to be controlled by the OC amount introduced by the percolating DOM solution and not by the spatial accessibility through soil pores. A coarse texture caused slight shifts in the microbial community toward drought tolerant species, without influencing the overall OC turnover under regular irrigation.

4.3 | Structure formation and stabilization by percolating dissolved OM

The percolating DOM was able to induce water-stable aggregates in all soils with a predominant formation of large macroaggregates (Figure 1A). Although mineral–mineral interactions accounted for the majority of the mineral surface coverage, this did not lead to significant changes in the size distribution of water-stable aggregates in the absence of DOM (Figure 1B). This implies that the biochemical processing of the available OM may induce the water-stable cohesion of mineral particles without requiring the presence of particulate OM nuclei. This is in line with previous experiments with artificial soils, where aggregate formation induced by DOM addition was observed in a clay-rich soil (Bucka et al., 2019). Moreover, the present experimental approach enabled the systematic assessment of the soil texture-effect separated from the effect of the mineral composition within the process of aggregate formation induced by a liquid OM source.

The mass transfer between the size fractions after the incubation highlights the overall importance of small particles for the aggregation process. The aggregation effect was strongest in the clay-rich soils (Figure 1B), with 58% of the particle mass being bound in the large macroaggregate fraction after the incubation (Figure 1A). If we compare the original particle size distribution of the mineral mixture, it can be shown that the newly formed macroaggregate fraction consisted of 90% newly added (finer) particles. This corresponds to a particle transfer of approx. 0.53 g to the largest aggregates per g soil. With higher sand contents in the soils (and correspondingly lower clay contents), this particle transfer was reduced, which led to a large macroaggregate fraction consisting of 66% newly added particles in the loam, and 47% newly added particles in the sandy loam. Translated to particle mass, this means that approx. 0.23 g moved to the largest aggregates per g soil, which is approx. half of the mass transferred in the clay-rich texture. This implies that the aggregation process requires the presence of small particles that can be connected by OM to larger aggregates independent of their surface charge.

Although the aggregation effect was strongest in the clay-rich soils, there was a significant macroaggregate formation even in the sand-rich soils (Figure 1B). This reveals that the biochemical processing of the DOM has the capacity to embed even sand-sized quartz grains into the aggregates, although the OC retention suggests the predominant adsorption of DOC to the surfaces of the clay minerals and the goethite, instead to the quartz. However, a close inspection of the mineral matrix revealed goethite-coated quartz in our artificial soils (Bucka, Felde, et al., 2021). Thus, the goethite may serve as bridge between quartz and OM, with the goethite coatings being attached to the quartz by covalent bounds (Scheidegger et al., 1993), and to the OM molecules via electrostatic forces (Dultz et al., 2018). A similar mechanism has already been suggested for goethite bridges between quartz and illite (Guhra et al., 2019). Considering the fact that goethite-masked sand grains can form large aggregates, this leads to the conclusion that the mineral composition of a soil adds to the effect of the soil texture with respect to aggregate formation. This expands our knowledge regarding soil structure formation, which is mostly based on the addition of particulate OM to natural topsoils (Denef et al., 2002), toward the effects of a liquid OM source within a subsoil context. In addition, our experiment underlines the relevance of sand-sized particles within the process of aggregate formation, which was only recently put into research focus (Bucka, Felde, et al., 2021; Felde et al., 2021; Paradiś et al., 2017).

The large macroaggregate fraction had the same OC content as the bulk soil in all textures, meaning no OC enrichment took place in this fraction (Figure 2). This suggests that the OC transfer to the largest aggregate fraction took place to the same extent as the mass transfer of finer particles. This underlines the importance of the fine particles for the formation of large aggregates, as they are connected by OM and thereby form larger aggregates. In addition, it proves that a relatively low amount of OC (0.7 ± 0.1 mg OC g^{-1}) is already sufficient to produce those large water-stable aggregates (Figure 2).

When the aggregates were crushed by mechanical force, the work required to break the aggregates down to 80% of their original size was highest in the clay-rich (0.11 ± 0.03 mJ mm^{-1}) and lowest in the sand-rich aggregates (0.06 ± 0.01 mJ mm^{-1}, Figure 3A), meaning that the aggregates formed in the clay-rich texture have a higher mechanical stability. This can be ascribed to the higher number of clay-sized particles, which enable more particle–particle contact points due to their greater surface area-to-mass ratio. However, the mechanical destruction by dry crushing revealed an overall lower mechanical stability for the artificially formed aggregates by DOM, than it has been observed in aggregates of natural, arable soils of comparable texture and mineral composition (Felde et al., 2021). This implies that the overall mechanical stability of a matured soil aggregate relies on additional stabilization factors, which the interaction of dissolved OM and mineral surfaces does not provide.

The breakdown pattern during the crushing revealed a smaller number of small force drops (<10%), and a larger number of large force drops (>40%) for the aggregates formed in sand-rich texture (Figure 3B). This suggests many large cracks that can be explained with the sand grains being split off at very low mechanical stress. In contrast, the clay-rich aggregates seem to be breaking down into a series of small microfractures, which is indicative of a relatively homogenous aggregate structure. These aggregates are possibly comprised of many small, interconnected particles with fine pores in between, causing a force resistant, but brittle structure.

The biochemical processing of the percolating DOM solution induced the formation of large aggregates in all textures without requiring the presence of particulate organic nuclei. However, the

presence of fine mineral particles fosters the formation of large aggregates, irrespective of their surface charge or sorptive properties. The aggregates' water-stability can be established by very low OC contents in various soil textures, whereas a higher clay-content was connected to a higher mechanical stability. The presence of goethite-coated sand grains within larger aggregates shows that the mineral composition of a soil adds to the effect of the soil texture with respect to aggregate formation.

5 | CONCLUSIONS

With our simulated subsoil environment, we closed the gap between batch experiments and natural soil studies by studying the biochemical processing of percolating dissolved OM under unsaturated flow conditions. This allowed disentangling the role of soil texture (i.e., grain size) and mineral composition for sorption and biochemical processing of DOM and initial structure formation.

Although the soil texture defined the pore space and the amount of retained soil solution, the effective OC retention from dissolved OM was decoupled from the movement of the soil solution. This suggests that the OC storage relies on the clay mineral composition enabling adsorption instead on relying on the amount of clay. A higher amount of clay-sized quartz may even "dilute" the available mineral surface area for OM sorption.

The microbial OC turnover was independent of the soil texture and its corresponding pore system. This suggests that the initial OC turnover in subsoils, where the main OM input comes from percolating DOM within an OC-free and unstructured mineral matrix, is controlled by the OC input and not by its spatial accessibility through soil pores.

A coarser soil texture induced slight shifts in the microbial community toward drought tolerant species, without influencing the overall OC turnover under regular irrigation.

The biochemical processing of the percolating DOM solution induced the formation of large aggregates in all soil textures without requiring the presence of particulate organic nuclei. However, the formation and mechanical stability of large aggregates was higher in the clay-rich mixtures, which implies that the emerging soil structure relies on the amount of fine mineral particles, irrespective of their surface charge or sorptive properties. The presence of goethite-coated sand grains within larger aggregates indicates that the mineral composition of a soil may add to the soil texture effect with respect to aggregate formation.

The results of our experiment highlight the need to separate the effects of soil texture (i.e., particle size) and clay mineral composition with respect to relevant subsoil processes regarding OC retention, microbial turnover, and soil structure formation at early development stages.

ACKNOWLEDGMENTS

The research was funded by the *Deutsche Forschungsgemeinschaft (DFG)* within the research unit *MAD Soil—Microaggregates: Formation and Turnover of the Structural Building Blocks of Soils* (*FOR 2179*). The authors gratefully acknowledge *Bärbel Deischl*, *Shu-Yin Tung*, *Gabriele Albert*, *Petra Bucher*, and *Christine Pfab* from the Technical University of Munich for their assistance with the lab work; *Vera Baumert* for establishing the PLFA extraction method in our group; *Pedro Paulo de C. Teixeira* and *Kristina Witzgall* for helpful discussions about the PLFA data; *Svenja Roosch* from the University of Hanover for the assistance with the dry crushing; *Angelika Kölbl* from the University Halle-Wittenberg for her ideas regarding the experimental setup.

Open access funding enabled and organized by Projekt DEAL.

DATA AVAILABILITY STATEMENT

The data that support the findings of this study are available from the corresponding author upon reasonable request.

ORCID

Franziska B. Bucka https://orcid.org/0000-0003-3922-8136
Vincent J. M. N. L. Felde https://orcid.org/0000-0002-1018-2376
Stephan Peth https://orcid.org/0000-0001-9799-212X

REFERENCES

Ahrens, B., Braakhekke, M. C., Guggenberger, G., Schrumpf, M., & Reichstein, M. (2015). Contribution of sorption, DOC transport and microbial interactions to the ^{14}C age of a soil organic carbon profile: Insights from a calibrated process model. *Soil Biology and Biochemistry*, *88*, 390–402.

Amato, M., & Ladd, J. N. (1992). Decomposition of ^{14}C-labelled glucose and legume material in soils: Properties influencing the accumulation of organic residue C and microbial biomass C. *Soil Biology and Biochemistry*, *24*(5), 455–464.

Amézketa, E. (1999). Soil aggregate stability: A review. *Journal of Sustainable Agriculture*, *14*(2–3), 83–151.

Angst, G., John, S., Mueller, C. W., Kögel-Knabner, I., & Rethemeyer, J. (2016). Tracing the sources and spatial distribution of organic carbon in subsoils using a multi-biomarker approach. *Scientific Reports*, *6*(1), 1–12.

Angst, G., Messinger, J., Greiner, M., Häusler, W., Hertel, D., Kirfel, K., Kögel-Knabner, I., Leuschner, C., Rethemeyer, J., & Mueller, C. W. (2018). Soil organic carbon stocks in topsoil and subsoil controlled by parent material, carbon input in the rhizosphere, and microbial-derived compounds. *Soil Biology and Biochemistry*, *122*, 19–30.

Barthès, B., & Roose, E. (2002). Aggregate stability as an indicator of soil susceptibility to runoff and erosion; validation at several levels. *Catena*, *47*(2), 133–149.

Batjes, N. H. (1996). Total carbon and nitrogen in the soils of the world. *European Journal of Soil Science*, *47*(2), 151–163.

Baumert, V. L., Vasilyeva, N. A., Vladimirov, A. A., Meier, I. C., Kögel-Knabner, I., & Mueller, C. W. (2018). Root exudates induce soil macroaggregation facilitated by fungi in subsoil. *Frontiers in Environmental Science*, *6*, 140. https://doi.org/10.3389/fenvs.2018.00140

Benard, P., Zarebanadkouki, M., Brax, M., Kaltenbach, R., Jerjen, I., Marone, F., Couradeau, E., Felde, V. J. M. N. L., Kaestner, A., & Carminati, A. (2019). Microhydrological niches in soils: How mucilage and EPS alter the biophysical properties of the rhizosphere and other biological hotspots. *Vadose Zone Journal*, *18*(1), 1–10.

Bimüller, C., Mueller, C. W., von Lützow, M., Kreyling, O., Kölbl, A., Haug, S., Schloter, M., & Kögel-Knabner, I. (2014). Decoupled carbon and nitrogen mineralization in soil particle size fractions of a forest topsoil. *Soil Biology and Biochemistry*, *78*, 263–273.

Brunauer, S., Emmett, P. H., & Teller, E. (1938). Adsorption of gases in multimolecular layers. *Journal of the American Chemical Society*, *60*(2), 309–319.

Bucka, F. B., Felde, V. J., Peth, S., & Kögel-Knabner, I. (2021). Disentangling the effects of OM quality and soil texture on microbially mediated structure formation in artificial model soils. *Geoderma*, *403*, 115213. https://doi.org/10.1016/j.geoderma.2021.115213

Bucka, F. B., Kölbl, A., Uteau, D., Peth, S., & Kögel-Knabner, I. (2019). Organic matter input determines structure development and aggregate formation in artificial soils. *Geoderma*, *354*, 113881. https://doi.org/10.1016/j.geoderma.2019.113881

Bucka, F. B., Pihlap, E., Kaiser, J., Baumgartl, T., & Kögel-Knabner, I. (2021). A small-scale test for rapid assessment of the soil development potential in post-mining soils. *Soil and Tillage Research*, *211*, 105016. https://doi.org/10.1016/j.still.2021.105016

Chabbi, A., Kögel-Knabner, I., & Rumpel, C. (2009). Stabilised carbon in subsoil horizons is located in spatially distinct parts of the soil profile. *Soil Biology and Biochemistry*, *41*(2), 256–261.

Christensen, B. T. (2000). Organic matter in soil-structure, function and turnover. (DIAS Report, Plant Production 2000 No. 30). Danish Institute of Agricultural Sciences, Research Center Foulum.

Costa, O. Y., Raaijmakers, J. M., & Kuramae, E. E. (2018). Microbial extracellular polymeric substances: Ecological function and impact on soil aggregation. *Frontiers in Microbiology*, *9*, 1636. https://doi.org/10.3389/fmicb.2018.01636

Dekker, L. W., & Ritsema, C. J. (2000). Wetting patterns and moisture variability in water repellent Dutch soils. *Journal of Hydrology*, *231*, 148–164.

Denef, K., Six, J., Merckx, R., & Paustian, K. (2002). Short-term effects of biological and physical forces on aggregate formation in soils with different clay mineralogy. *Plant and Soil*, *246*, 185–200.

Dexter, A. R. (1977). A statistical measure of the structure of tilled soil. *Journal of Agricultural Engineering Research*, *22*(1), 101–104.

Dexter, A. R. (1988). Advances in characterization of soil structure. *Soil and Tillage Research*, *11*(3–4), 199–238.

Dultz, S., Steinke, H., Mikutta, R., Woche, S. K., & Guggenberger, G. (2018). Impact of organic matter types on surface charge and aggregation of goethite. *Colloids and Surfaces A: Physicochemical and Engineering Aspects*, *554*, 156–168.

Felde, V. J., Schweizer, S. A., Biesgen, D., Ulbrich, A., Uteau, D., Knief, C., Graf-Rosenfellner, M., Kögel-Knabner, I., & Peth, S. (2021). Wet sieving versus dry crushing: Soil microaggregates reveal different physical structure, bacterial diversity and organic matter composition in a clay gradient. *European Journal of Soil Science*, *72*(2), 810–828.

Flemming, H. C., & Wingender, J. (2010). The biofilm matrix. *Nature Reviews Microbiology*, *8*(9), 623–633.

Franzluebbers, A. J. (2002). Water infiltration and soil structure related to organic matter and its stratification with depth. *Soil and Tillage Research*, *66*(2), 197–205.

Frostegård, Å., Tunlid, A., & Bååth, E. (1991). Microbial biomass measured as total lipid phosphate in soils of different organic content. *Journal of Microbiological Methods*, *14*(3), 151–163.

Frostegård, Å., Tunlid, A., & Bååth, E. (1993). Phospholipid fatty acid composition, biomass, and activity of microbial communities from two soil types experimentally exposed to different heavy metals. *Applied and Environmental Microbiology*, *59*(11), 3605–3617.

Guhra, T., Ritschel, T., & Totsche, K. U. (2019). Formation of mineral–mineral and organo–mineral composite building units from microaggregate-forming materials including microbially produced extracellular polymeric substances. *European Journal of Soil Science*, *70*(3), 604–615.

Hagedorn, F., & Machwitz, M. (2007). Controls on dissolved organic matter leaching from forest litter grown under elevated atmospheric CO_2. *Soil Biology and Biochemistry*, *39*(7), 1759–1769.

Hassink, J. (1997). The capacity of soils to preserve organic C and N by their association with clay and silt particles. *Plant and Soil*, *191*, 77–87.

Heister, K. (2014). The measurement of the specific surface area of soils by gas and polar liquid adsorption methods—Limitations and potentials. *Geoderma*, *216*, 75–87.

Heister, K. (2016). How accessible is the specific surface area of minerals? A comparative study with Al-containing minerals as model substances. *Geoderma*, *263*, 8–15.

Inagaki, T. M., Possinger, A. R., Grant, K. E., Schweizer, S. A., Mueller, C. W., Derry, L. A., Lehmann, J., & Kögel-Knabner, I. (2020). Subsoil organo-mineral associations under contrasting climate conditions. *Geochimica et Cosmochimica Acta*, *270*, 244–263.

Isermeyer, H. (1952). Eine einfache Methode zur Bestimmung der Bodenatmung und der Karbonate im Boden. *Zeitschrift für Pflanzenernährung, Düngung, Bodenkunde*, *56*(1–3), 26–38.

Jobbágy, E. G., & Jackson, R. B. (2000). The vertical distribution of soil organic carbon and its relation to climate and vegetation. *Ecological Applications*, *10*(2), 423–436.

Kahle, M., Kleber, M., & Jahn, R. (2003). Retention of dissolved organic matter by illitic soils and clay fractions: Influence of mineral phase properties. *Journal of Plant Nutrition and Soil Science*, *166*(6), 737–741.

Kaiser, K., & Guggenberger, G. (2003). Mineral surfaces and soil organic matter. *European Journal of Soil Science*, *54*(2), 219–236.

Kaiser, K., Guggenberger, G., & Haumaier, L. (2004). Changes in dissolved lignin-derived phenols, neutral sugars, uronic acids, and amino sugars with depth in forested Haplic Arenosols and Rendzic Leptosols. *Biogeochemistry*, *70*, 135–151.

Kaiser, K., Guggenberger, G., Haumaier, L., & Zech, W. (1997). Dissolved organic matter sorption on sub soils and minerals studied by ^{13}C-NMR and DRIFT spectroscopy. *European Journal of Soil Science*, *48*(2), 301–310.

Kaiser, K., & Kalbitz, K. (2012). Cycling downwards–dissolved organic matter in soils. *Soil Biology and Biochemistry*, *52*, 29–32.

Kalbitz, K., Solinger, S., Park, J. H., Michalzik, B., & Matzner, E. (2000). Controls on the dynamics of dissolved organic matter in soils: A review. *Soil Science*, *165*(4), 277–304.

Knicker, H., González-Vila, F. J., Polvillo, O., González, J. A., & Almendros, G. (2005). Fire-induced transformation of C-and N-forms in different organic soil fractions from a Dystric Cambisol under a Mediterranean pine forest (*Pinus pinaster*). *Soil Biology and Biochemistry*, *37*(4), 701–718.

Kögel-Knabner, I. (2002). The macromolecular organic composition of plant and microbial residues as inputs to soil organic matter. *Soil Biology and Biochemistry*, *34*(2), 139–162.

Kögel-Knabner, I., & Amelung, W. (2021). Soil organic matter in major pedogenic soil groups. *Geoderma*, *384*, 114785. https://doi.org/10.1016/j.geoderma.2020.114785

Krettek, A., & Rennert, T. (2021). Mobilisation of Al, Fe, and DOM from topsoil during simulated early Podzol development and subsequent DOM adsorption on model minerals. *Scientific Reports*, *11*(1), 19741. https://doi.org/10.1038/s41598-021-99365-y

Ladd, J. N., Amato, M., & Oades, J. M. (1985). Decomposition of plant material in Australian soils. III. Residual organic and microbial biomass C and N from isotope-labelled legume material and soil organic matter, decomposing under field conditions. *Soil Research*, *23*(4), 603–611.

Lehmann, J., Solomon, D., Kinyangi, J., Dathe, L., Wirick, S., & Jacobsen, C. (2008). Spatial complexity of soil organic matter forms at nanometre scales. *Nature Geoscience*, *1*(4), 238–242.

Lehmann, K., Schaefer, S., Babin, D., Köhne, J. M., Schlüter, S., Smalla, K., Vogel, H.-J., & Totsche, K. U. (2018). Selective transport and retention of organic matter and bacteria shapes initial pedogenesis in artificial soil-a two-layer column study. *Geoderma*, *325*, 37–48.

Liu, H., Wu, Y., Ai, Z., Zhang, J., Zhang, C., Xue, S., & Liu, G. (2019). Effects of the interaction between temperature and revegetation on the microbial degradation of soil dissolved organic matter (DOM)—A DOM incubation experiment. *Geoderma*, *337*, 812–824.

Lorenz, K., & Lal, R. (2005). The depth distribution of soil organic carbon in relation to land use and management and the potential of carbon sequestration in subsoil horizons. *Advances in Agronomy*, *88*, 35–66.

McCarthy, J. F. (2005). Carbon fluxes in soil: Long-term sequestration in deeper soil horizons. *Journal of Geographical Sciences*, *15*, 149–154.

Merdy, P., Lucas, Y., Coulomb, B., Melfi, A. J., & Montes, C. R. (2021). Soil organic carbon mobility in equatorial podzols: Soil column experiments. *Soil*, *7*(2), 585–594.

Meyer, N., Welp, G., Rodionov, A., Borchard, N., Martius, C., & Amelung, W. (2018). Nitrogen and phosphorus supply controls soil organic carbon mineralization in tropical topsoil and subsoil. *Soil Biology and Biochemistry*, *119*, 152–161.

Mikutta, R., Mikutta, C., Kalbitz, K., Scheel, T., Kaiser, K., & Jahn, R. (2007). Biodegradation of forest floor organic matter bound to minerals via different binding mechanisms. *Geochimica et Cosmochimica Acta*, *71*(10), 2569–2590.

Mikutta, R., Turner, S., Schippers, A., Gentsch, N., Meyer-Stüve, S., Condron, L. M., Peltzer, D. A., Richardson, S. J., Eger, A., Hempel, G., Kaiser, K., Klotzbücher, T., & Guggenberger, G. (2019). Microbial and abiotic controls on mineral-associated organic matter in soil profiles along an ecosystem gradient. *Scientific Reports*, *9*(1), 10294. https://doi.org/10.1038/s41598-019-46501-4

Morales, V. L., Parlange, J. Y., & Steenhuis, T. S. (2010). Are preferential flow paths perpetuated by microbial activity in the soil matrix? A review. *Journal of Hydrology*, *393*(1–2), 29–36.

Nelson, P. N., Baldock, J. A., & Oades, J. M. (1992). Concentration and composition of dissolved organic carbon in streams in relation to catchment soil properties. *Biogeochemistry*, *19*, 27–50.

Nelson, P. N., & Baldock, J. A. (2005). Estimating the molecular composition of a diverse range of natural organic materials from solid-state ^{13}C NMR and elemental analyses. *Biogeochemistry*, *72*, 1–34.

Otten, W., Gilligan, C. A., Watts, C. W., Dexter, A. R., & Hall, D. (1999). Continuity of air-filled pores and invasion thresholds for a soil-borne fungal plant pathogen, *Rhizoctonia solani*. *Soil Biology and Biochemistry*, *31*(13), 1803–1810.

Paradiś, A., Brueck, C., Meisenheimer, D., Wanzek, T., & Dragila, M. I. (2017). Sandy soil microaggregates: Rethinking our understanding of hydraulic function. *Vadose Zone Journal*, *16*(9), 1–10.

Pronk, G. J., Heister, K., Ding, G. C., Smalla, K., & Kögel-Knabner, I. (2012). Development of biogeochemical interfaces in an artificial soil incubation experiment; aggregation and formation of organo-mineral associations. *Geoderma*, *189*, 585–594.

Qualls, R. G., & Haines, B. L. (1992). Biodegradability of dissolved organic matter in forest throughfall, soil solution, and stream water. *Soil Science Society of America Journal*, *56*(2), 578–586.

R Core Team. (2017). *R: A language and environment for statistical computing*. R Foundation. https://www.R-project.org/

Roberson, E. B., & Firestone, M. K. (1992). Relationship between desiccation and exopolysaccharide production in a soil *Pseudomonas* sp. *Applied and Environmental Microbiology*, *58*(4), 1284–1291.

Rumpel, C., Chabbi, A., & Marschner, B. (2012). Carbon storage and sequestration in subsoil horizons: Knowledge, gaps and potentials. In R. Lal, K. Lorenz, R. F. Hüttl, B. U. Schneider, & J. von Braun (Eds.), *Recarbonization of the biosphere* (pp. 445–464). Springer.

Rumpel, C., & Kögel-Knabner, I. (2011). Deep soil organic matter—A key but poorly understood component of terrestrial C cycle. *Plant and Soil*, *338*, 143–158.

Schaefer, J., & Stejskal, E. O. (1976). Carbon-13 nuclear magnetic resonance of polymers spinning at the magic angle. *Journal of the American Chemical Society*, *98*(4), 1031–1032.

Scheidegger, A., Borkovec, M., & Sticher, H. (1993). Coating of silica sand with goethite: Preparation and analytical identification. *Geoderma*, *58*(1–2), 43–65.

Schimel, J., Balser, T. C., & Wallenstein, M. (2007). Microbial stress-response physiology and its implications for ecosystem function. *Ecology*, *88*(6), 1386–1394.

Shen, Y. H. (1999). Sorption of natural dissolved organic matter on soil. *Chemosphere*, *38*(7), 1505–1515.

Sokol, N. W., Sanderman, J., & Bradford, M. A. (2019). Pathways of mineral-associated soil organic matter formation: Integrating the role of plant carbon source, chemistry, and point of entry. *Global Change Biology*, *25*(1), 12–24.

Sørensen, L. H. (1972). Stabilization of newly formed amino acid metabolites in soil by clay minerals. *Soil Science*, *114*(1), 5–11.

Soufan, R., Delaunay, Y., Gonod, L. V., Shor, L. M., Garnier, P., Otten, W., & Baveye, P. C. (2018). Pore-scale monitoring of the effect of microarchitecture on fungal growth in a two-dimensional soil-like micromodel. *Frontiers in Environmental Science*, *6*, 68. https://doi.org/10.3389/fenvs.2018.00068

Thomsen, I. K., Schjønning, P., Jensen, B., Kristensen, K., & Christensen, B. T. (1999). Turnover of organic matter in differently textured soils: II. Microbial activity as influenced by soil water regimes. *Geoderma*, *89*(3–4), 199–218.

Tisdall, J. M. (2020). Formation of soil aggregates and accumulation of soil organic matter. In M. R. Carter, & B. A Stewart (Ed.), *Structure and organic matter storage in agricultural soils* (pp. 57–96). CRC Press.

Tisdall, J. M., & OADES, J. M. (1982). Organic matter and water-stable aggregates in soils. *Journal of Soil Science*, *33*(2), 141–163.

Totsche, K. U., Amelung, W., Gerzabek, M. H., Guggenberger, G., Klumpp, E., Knief, C., Lehndorff, E., Mikutta, R., Peth, S., Prechtel, A., Ray, N., & Kögel-Knabner, I. (2018). Microaggregates in soils. *Journal of Plant Nutrition and Soil Science*, *181*(1), 104–136.

Tuller, M., Or, D., & Hillel, D. (2004). Retention of water in soil and the soil water characteristic curve. *Encyclopedia of Soils in the Environment*, *4*, 278–289.

Wagai, R., Mayer, L. M., & Kitayama, K. (2009). Extent and nature of organic coverage of soil mineral surfaces assessed by a gas sorption approach. *Geoderma*, *149*(1–2), 152–160.

Weigand, H., & Totsche, K. U. (1998). Flow and reactivity effects on dissolved organic matter transport in soil columns. *Soil Science Society of America Journal*, *62*(5), 1268–1274.

Wilson, M. (1987). *NMR techniques and applications in geochemistry and soil chemistry*. Cambridge University Press.

Witzgall, K., Vidal, A., Schubert, D. I., Höschen, C., Schweizer, S. A., Buegger, F., Pouteau, V., Chenu, C., & Mueller, C. W. (2021). Particulate organic matter as a functional soil component for persistent soil organic carbon. *Nature Communications*, *12*(1), 4115. https://doi.org/10.1038/s41467-021-24192-8

SUPPORTING INFORMATION

Additional supporting information can be found online in the Supporting Information section at the end of this article.

How to cite this article: Bucka, F. B., Felde, V. J. M. N. L., Peth, S., & Kögel-Knabner, I. (2024). Complementary effects of sorption and biochemical processing of dissolved organic matter for emerging structure formation controlled by soil texture. *Journal of Plant Nutrition and Soil Science*, *187*, 51–62. https://doi.org/10.1002/jpln.202200391